

# Decadal Trends and Variability in SSM/I Brightness Temperatures and Earth Incidence Angle

Kyle Hilburn, Remote Sensing Systems (hilburn@remss.com)  
Chung-Lin Shie, UMBC/JCET, NASA/GSFC

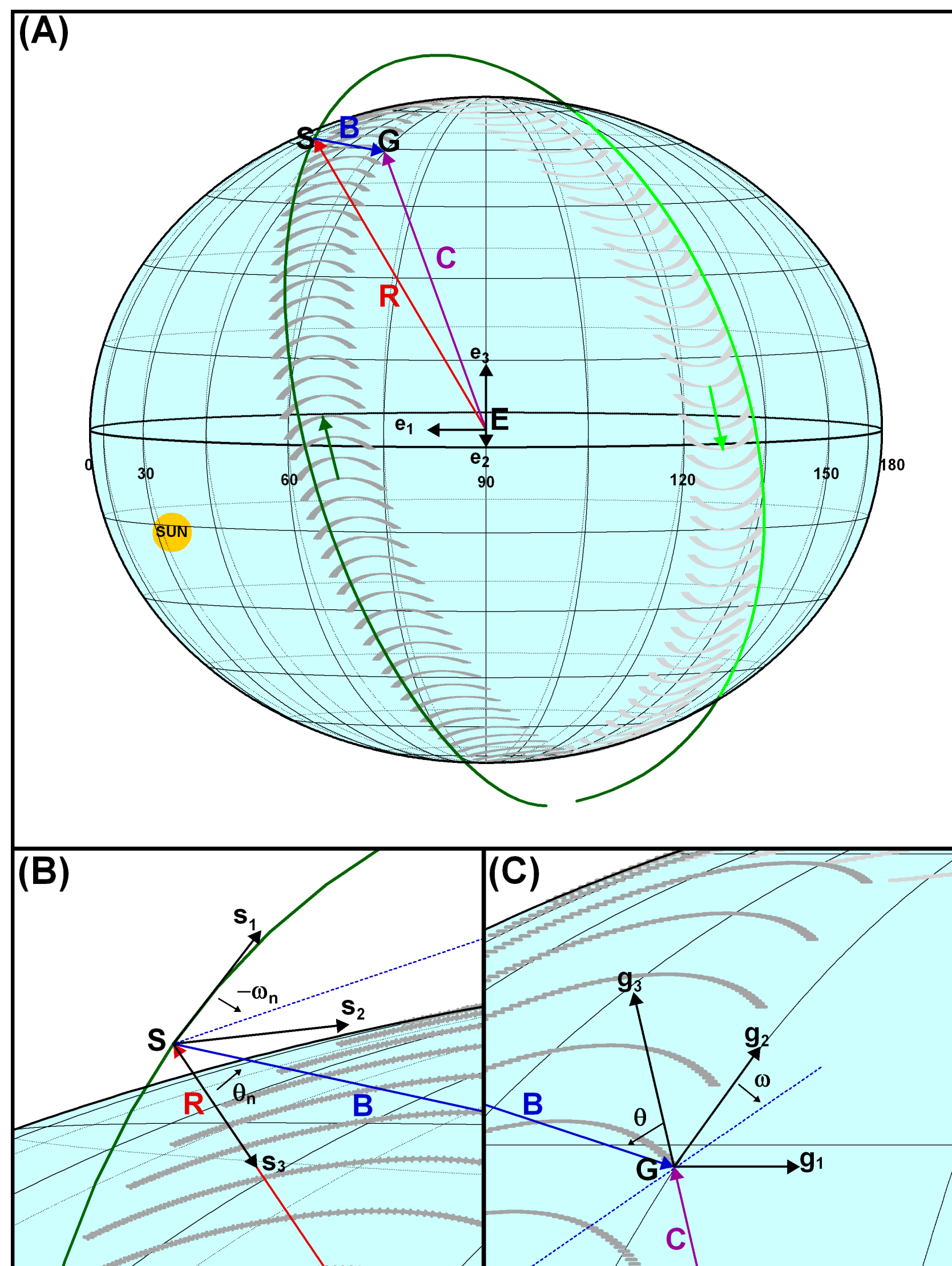
Remote Sensing Systems  
www.remss.com

## 1. INTRODUCTION

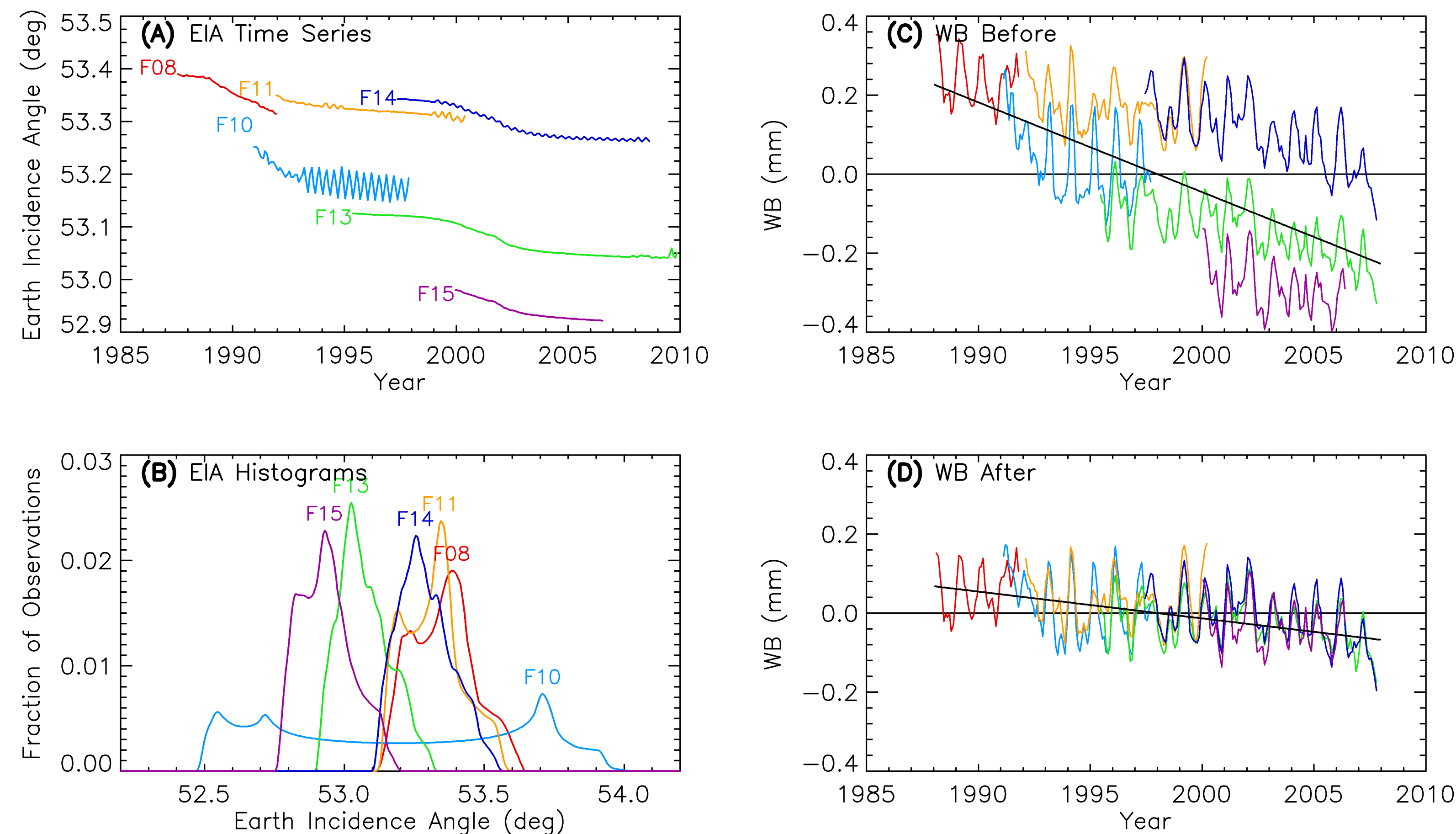
Chung-Lin Shie produces the Goddard Satellite-based Surface Turbulent Fluxes (GSSTF) dataset using Remote Sensing Systems (RSS) Special Sensor Microwave / Imager (SSM/I) brightness temperature  $T_B$  dataset. The latent heat flux calculation in GSSTF depends on the lowest 500-m bottom-layer water vapor  $W_B$ ; calculated using the Schulz et al. (1993) relationship:  $W_B(\text{mm}) = -59.339 + 0.3697 \cdot T_{19V} - 0.2390 \cdot T_{19H} + 0.1559 \cdot T_{22V} - 0.0497 \cdot T_{37V}$ .

Chung-Lin found a surprising result: while the trend in total water vapor is about +1% per decade; the trend in  $W_B$  was -4% per decade. Through collaboration, we determined the  $W_B$  trend was due to trends and inter-satellite variability in the Earth incidence angle (EIA). RSS has always removed EIA effects from its geophysical retrievals using its geophysical retrieval algorithms, without altering the  $T_B$  in the SSM/I dataset. To use the  $W_B$  retrieval above, which does not account for EIA, a simple and accurate method for removing EIA effects from  $T_B$  is needed. This poster describes our major results. Complete details including the correction coefficients are given in Hilburn and Shie (2011), available at: [http://www.remss.com/support/rss\\_tech\\_reports\\_by\\_year.html](http://www.remss.com/support/rss_tech_reports_by_year.html).

The schematic, based on one orbit of F13 SSM/I data, depicts EIA geometry. There are three coordinate systems: Earth (**Panel A**), satellite (**Panel B**), and the location where the boresight vector intersects the ground (**Panel C**). For a satellite flying a geodetic mission, the EIA (angle  $\theta$  in **Panel C**) depends primarily on the altitude of the satellite (vector  $R$  in **Panel A**) and the angle of the boresight vector relative to nadir (angle  $\theta_n$  in **Panel B**), which is constant for each SSM/I sensor.



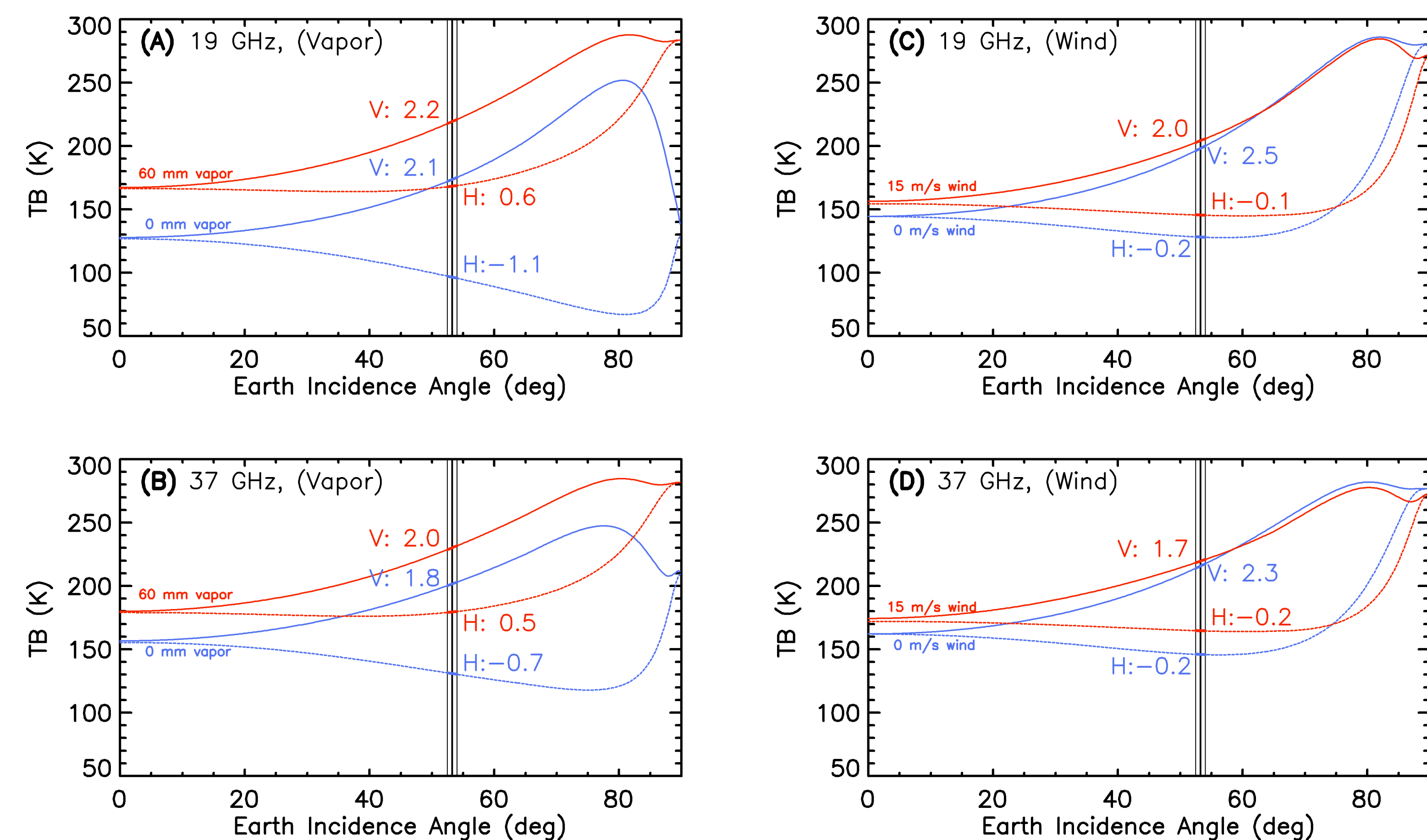
## 2. INCIDENCE ANGLE VARIABILITY



**Panel A:** EIA time series for all six SSM/I. Inter-satellite offsets and downward trends can be seen. The trends are due to decreasing altitude. **Panel B:** EIA histograms for each SSM/I. The histograms are accurately modeled with the sum of four sources of variability, in order of period: scan position ( $\pm 0.01^\circ$  per 1.9 sec), orbit position ( $\pm 0.1^\circ$  per 101 minutes), perigee angle ( $\pm 0.1^\circ$  per 125 days, larger for F10), and long-term trends ( $-0.14^\circ$  per decade). The precession of perigee (also known as apsidal precession) is a rotation of the whole orbit in the orbital plane. It occurs because the earth is an oblate spheroid. This is the cause of the oscillations in the EIA time series in **Panel A**, which are especially evident for F10.

Time series of  $W_B$  before (**Panel C**) and after (**Panel D**) applying our EIA correction. The correction removes the inter-satellite offsets and trends. The overall trend is increased by 3% per decade. A small downward trend remains in the corrected  $W_B$  time series, and further research is necessary before a definitive statement of  $W_B$  trend accuracy can be made.

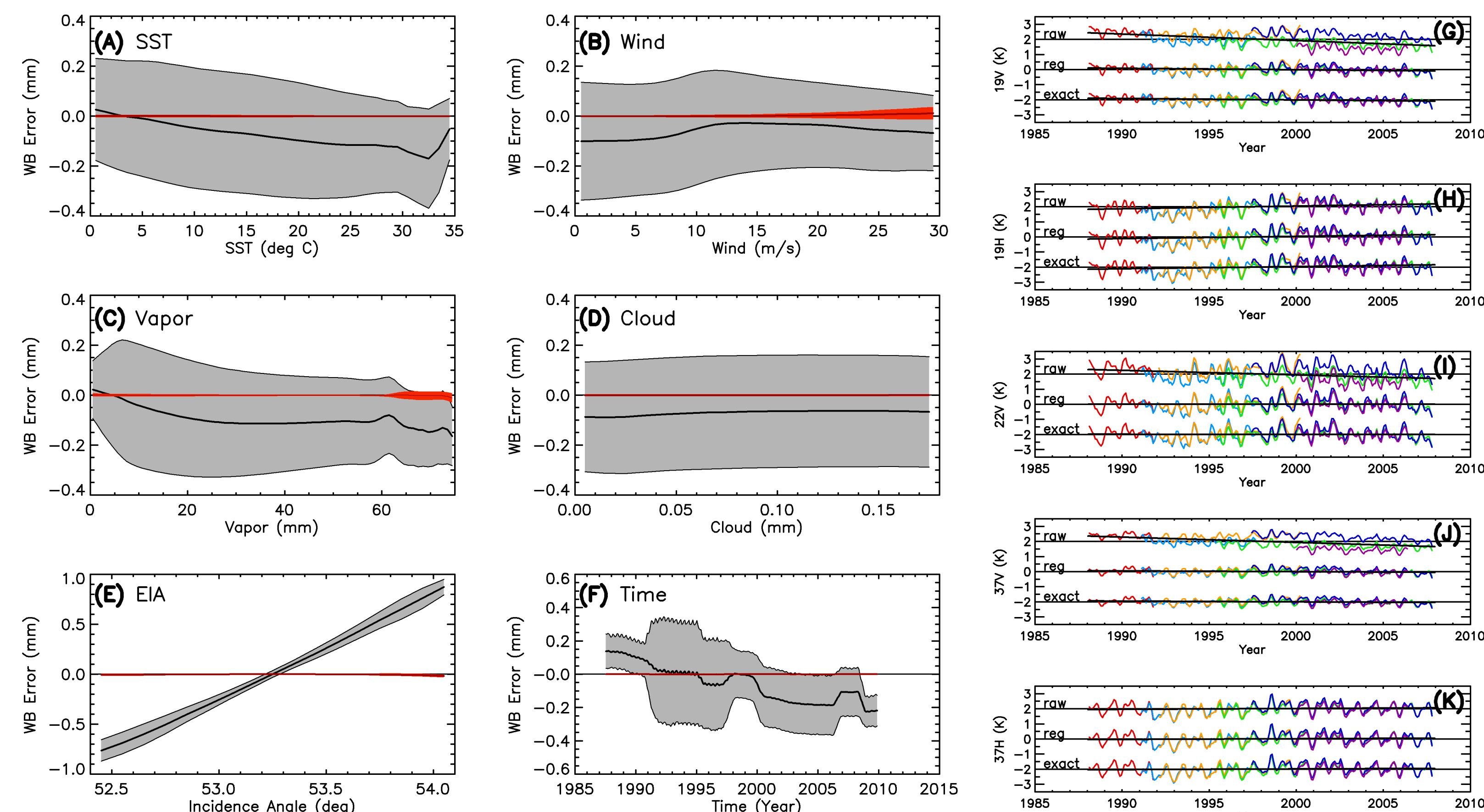
## 3. EFFECT ON BRIGHTNESS TEMPERATURE



All four panels illustrate the brightness temperature dependence on EIA. The range of EIAs observed by SSM/I are indicated by the vertical lines. The numbers on the plot are values of the derivative  $dT_B/d\theta$  with units of K/deg. **Panel A** (19 GHz) and **Panel B** (37 GHz) both compare the derivative for 0 mm water vapor (blue) and 60 mm water vapor (red). The H-pol derivative varies strongly with vapor, while V-pol does not. **Panel C** (19 GHz) and **Panel D** (37 GHz) both compare the derivative for 0 m/s wind speed (blue) and 15 m/s wind speed (red). The V-pol derivative varies modestly with wind speed, while H-pol does not. **Panels A** and **B** assume a wind speed of 7 m/s, and **Panels C** and **D** assume a water vapor of 30 mm.

$T_B$  can be referenced to a nominal incidence angle with a Taylor series expansion. This requires knowing the change in  $T_B$  with EIA. Over the rain-free ocean, this derivative depends on: frequency, polarization, EIA, sea surface temperature, surface wind speed and direction, columnar water vapor, and columnar cloud water. We specified the derivative using the RSS radiative transfer model and derived a regression relationship in terms of  $T_B$ . Please see Hilburn and Shie (2011) for more details.

## 4. RESULTS AND CONCLUSIONS



**Panels (A) through (F)** show the accuracy of our correction for  $W_B$  as a function of: **(A)** sea surface temperature, **(B)** wind speed, **(C)** water vapor, **(D)** cloud water, **(E)** EIA, and **(F)** time. The black lines and grey envelopes indicate the mean and standard deviation before correction. The dark red lines and light red envelopes indicate the mean and standard deviation after applying our regression-based correction. In both cases, the differences are relative to an exact correction made using the full RSS radiative transfer model. Overall,  $W_B$  has an RMS error of 0.239 mm before correcting for EIA variability. The regression-based correction lowers this to 0.004 mm. Our correction provides highly accurate results over all physical conditions and at a level accurate for climate trend analysis. The correction has been implemented in the recently completed GSSTF Version-2c (GSSTF2c) that is scheduled for an official distribution via NASA GES DISC by October 2011.

**Panels (G) through (K)** show the effect of the correction on time series of  $T_B$ : **(G)** 19V, **(H)** 19H, **(I)** 22V, **(J)** 37V, and **(K)** 37H. In all of these panels, the top set of curves (+2 K) are uncorrected, the middle set were corrected using our regression, and the bottom set (-2 K) were corrected using an exact adjustment from the RSS RTM. A brightness temperature observation fundamentally depends on the Earth incidence angle of the observation. Legacy algorithms that do not include this dependence will have large inter-satellite offsets and spurious long-term trends. Globally on average,  $dT_B/d\theta$  is about 2 K/deg for V-pol and 0 K/deg for H-pol. Overall, SSM/I has an EIA trend of  $-0.14^\circ$  per decade. This produces a trend in V-pol  $T_B$  of about -0.3 K per decade. For the Schulz  $W_B$  algorithm, which does not account for EIA, this produces a spurious -3% per decade trend in  $W_B$ .